Int. J. Heat Mass Transfer. Vol. 22, pp. 1577–1585.

0017–9310/79/1101–1577 $02.00/0

HEAT AND MASS TRANSFER IN A SATURATED POROUS WEDGE WITH IMPERMEABLE BOUNDARIES

K. P. GOYAL* and D. R. KASSOY
Mechanical Engineering Department, University of Colorado, Boulder, CO 80309, U.S.A.

(*Received* 14 *November* 1978 *and in revised form* 16 *March* 1979)

Abstract—Heat and mass transfer in a two-dimensional radial flow of a viscous fluid through a saturated porous wedge-shaped region with confining walls is studied. Similarity transformations are used for the temperature, velocity and pressure, in order to reduce the describing systems to ordinary differential equations with two-point boundary conditions. Both exact and asymptotic solutions are obtained for the velocity and the temperature. It is found that two distinct solutions (jet flow type and slug flow type) exist for a given set of flow parameters. Specific results are presented for small wedge angles. It is shown that symmetric diverging solutions do not exist above a critical Rayleigh number. An application of the theory to the convection of liquid water in a crude model of a fault zone in a geothermally active area is presented.

NOMENCLATURE

Dimensional quantities carry a prime, while non-dimensional quantities do not.

- b, extent of fault zone perpendicular to plane of flow;
- c_{p0}, reference specific heat at constant pressure;
- $\mathbf{e}_3$, unit vector in the vertical direction;
- F, similarity temperature, a pure function of $\theta = Tr^{1/(1+\alpha)}$;
- g, gravity constant;
- G, similarity velocity, a pure function of $\theta = rV_r$;
- k_0, reference permeability of the medium;
- L, characteristic length [defined in equation (41)];
- M, mass flow rate;
- P, isotropic pressure, over pressure in the wedge;
- P_H, hydrostatic pressure corresponding to the density ρ_0;
- r, radial distance from the apex of the wedge;
- S, similarity pressure, a pure function of $\theta = Pr^{-\alpha/(1+\alpha)}$;
- T, temperature at any point in the wedge;
- T_{max}, maximum temperature in the wedge, specified at $r = 1$;
- T_0, reference temperature;
- $\mathbf{v}$, Darcy velocity vector times density;
- v_r, radial component of $\mathbf{v}$;
- v_θ, tangential component of $\mathbf{v}$.

Greek symbols

- α, exponent of T;
- α_{e0}, reference coefficient of thermal expansion;
- ΔT, characteristic temperature difference in the system [defined in equation (39)];
- ∇, del operator;
- θ_e, semi-wedge angle;
- λ_{m0}, reference thermal conductivity of the medium;
- μ_0, reference viscosity of the fluid;
- ν, kinematic viscosity;
- ν_0, reference kinematic viscosity;
- ρ, density;
- ρ_0, reference density.

1. INTRODUCTION

STUDIES of continuous viscous flow between non-parallel plane walls have been of interest since Jeffery [7] and Hamel [5] found the exact solutions of the hydrodynamic equations. Harrison [6], Karman [9], Tollmien [17], Noether [15] and Dean [1] dealt with specialized applications of the problem. A systematic treatment of the general problem was developed by Rosenhead [16], who presented similarity-type solutions for different Reynolds numbers and wedge angles. Millsaps and Pohlhausen [13] described the energy transfer associated with the Jeffery–Hamel hydrodynamic problem. Much later, Fraenkel [2, 3] showed that the nonuniqueness properties of the describing mathematical system lead to the appearance of additional solutions.

Katkov [11] showed that the exact similarity formulation could be extended to include free convection if the Boussinesq approximation is used in the momentum equation, if the dissipation term in the energy equation is negligible, and if the transport properties are constant. In this case, the wall temperatures must be proportional to the reciprocal of the radial distance cubed. Lu and Chen [12] developed solutions to the problem formulated by Katkov [11]. Both convergent and divergent flow

*Present address: Earth Sciences Division, Building 90, Lawrence Berkeley Laboratory, University of California, Berkeley, CA 94720, U.S.A.

solutions for different values of Reynolds number and Prandtl numbers are presented.

In the present work, we develop exact solutions for the equations which describe the flow of a liquid in a saturated porous medium. It is assumed that mass enters the apex of a wedge-shaped region (Fig. 1) bounded by impermeable walls, at the rate M'. The boundary temperature decreases with distance from the apex at a rate consistent with the similarity theory used to construct solutions. The thermal conductivity of the saturated medium, the liquid specific heat and the thermal expansion coefficient are constant. Similarity analysis requirements imply that the liquid viscosity decreases with increasing temperatures. This property is not unlike that of water, in which a temperature change from 25 to 225°C causes an 8-fold decrease in the viscosity. The porous medium is assumed to be isotropic and homogeneous. It follows that the porosity and permeability are constant. We examine the effect of buoyancy on the steady forced convection in a wedge-shaped region. Radial flow conditions are invoked so that similarity theory can be employed to find exact solutions. The basic mathematical system is reduced to a coupled set of ordinary differential equations with two-point boundary conditions. A combination of numerical and analytical methods is used to solve these equations. The results presented here are for a slender wedge configuration when $\theta_e \ll 1$. Additional results for other parameter values can be found in Goyal [4]. The theory is used to calculate heat and mass transport in a crude model of a fault zone in the earth's crust in a manner similar to that of Kassoy and Zebib [10], who considered the cooling of a rising column of hot liquid in a saturated porous medium within a channel confined by impermeable walls.

2. DESCRIBING EQUATIONS

The non-dimensional governing equations are

$$\nabla \cdot \mathbf{v} = 0, \tag{1}$$

$$v\mathbf{v} = T\mathbf{e}_3 - \nabla P, \tag{2}$$

$$R\mathbf{v} \cdot \nabla T = \nabla^2 T, \tag{3}$$

where

$$\mathbf{v} = \frac{\rho' \text{ (Darcy velocity vector)}}{\alpha'_{e0}\Delta T' g' k'_0 \rho'^2_0/\mu'_0}, \tag{4a}$$

$$v(T) = \frac{\nu'}{\nu'_0}, \quad T = \frac{T' - T'_0}{\Delta T'}, \tag{4b,c}$$

$$P = \frac{P' - P'_H}{\rho'_0 g' L' \alpha e'_0 \Delta T'}, \; r = \frac{r'}{L'}, \; 1 \leqslant r \leqslant \infty, \tag{4d,e}$$

$$R = \text{Rayleigh number} = \frac{L'\Delta T' g' \alpha'_{e0} k'_0 c'_{p0} \mu'_0}{\nu'^2_0 \lambda'_{m0}}. \tag{4f}$$

On the impermeable boundaries the normal component of the velocity must vanish and the

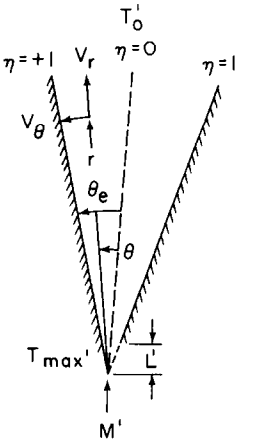

FIG. 1. The wedge-shaped region.

temperature decreases with increasing radial distance from the origin at a rate compatible with the similarity theory used for solution development. Mass flux at any constant radial coordinate is equivalent to that entering the wedge at the apex. If

$$\nu = T^{-\alpha}, \quad \alpha \geqslant 0, \tag{5}$$

then equations (1)–(3) can be reduced to ordinary differential equations by using the following similarity transformations:

$$v_r = \frac{G(\theta)}{r}, \tag{6}$$

$$v_\theta = 0, \tag{7}$$

$$T = \frac{F(\theta)}{r^{1/(1+\alpha)}}, \tag{8}$$

$$P = r^{\alpha/(1+\alpha)} S(\theta). \tag{9}$$

Equation (1) is satisfied identically. The coupled equations describing F and G can be written as,

$$\frac{dG}{d\eta} = \frac{d}{d\eta}\left[\frac{\cos(\theta_e \eta)}{\alpha+1} F^{\alpha+1}\right] + \frac{\alpha G}{F}\frac{dF}{d\eta}, \tag{10}$$

$$\frac{d^2F}{d\eta^2} + \frac{\theta_e^2 F}{(1+\alpha)^2} = -\frac{R_\theta F G}{\alpha+1}, \tag{11}$$

where

$$\eta = \frac{\theta}{\theta_e}, \quad R_\theta = R\theta_e^2. \tag{12}$$

Solutions to equations (10) and (11) are subjected to the following boundary conditions:

$$F(\eta = 1) = 1, \quad \frac{dF}{d\eta}(\eta = 0) = 0, \quad M = \int_0^1 G \, d\eta, \tag{13a,b,c}$$

where

$$M = \frac{M'}{2\rho'_0 \alpha'_{e0} \Delta T' g' k'_0 L' \theta_e / \nu'_0}. \tag{14}$$

Equations (8) and (13a) imply that the boundary temperature varies like $r^{-1/(1+\alpha)}$. Flow symmetry is

imposed by equation (13b). Global mass conservation is expressed by equation (13c). The singularity at $r = 0$ is similar to that found in theories of this generic type. Once F and G are found, the pressure field can be obtained from (2) and (9).

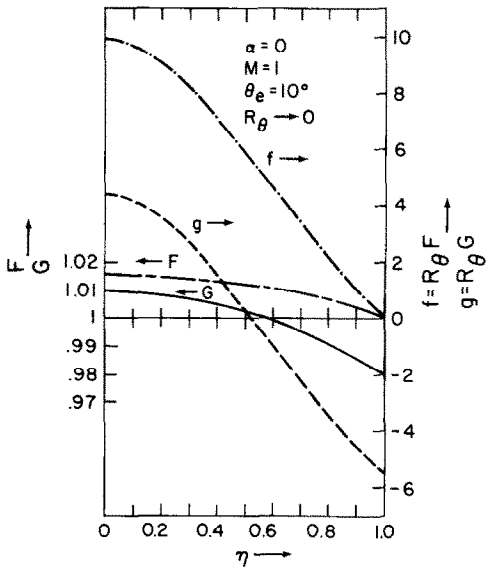

FIG. 2. Slug flow (F, G) and jet flow (f, g) solutions as a function of the nondimensional wedge angle (η): $\alpha = 0$, $M = 1$, $\theta_e = 10°$, $R_\theta \to 0$.

3. ASYMPTOTIC ANALYSIS

Asymptotic methods can be used to facilitate solution development when the paramcters R_θ and θ_e have certain special values. Low Rayleigh number solutions $(R \to 0)$ can be obtained from the limit $R_\theta \to 0$, θ_e fixed. When $F = O(1)$ and $G = O(1)$, the lowest-order solutions for $\alpha = 0$ (constant kinematic viscosity) are given as follows:

$$F(\eta) = \cos(\theta_e \eta)/\cos\theta_e, \tag{15}$$

$$G(\eta) = \frac{\cos(2\theta_e\eta)}{2\cos\theta_e} + M - \frac{\sin\theta_e}{2\theta_e}, \quad \theta_e < \pi/2. \tag{16}$$

In the case of a slender wedge, $\theta_e \ll 1$,

$$F \approx 1, \quad G \approx M, \tag{17}$$

implying isothermal slug flow. Thermally induced variations are enhanced by increasing θ_e. Both F and G decrease monotonically from $\eta = 0$ to $\eta = 1$ for any value of θ_e (Fig. 2).

A second class of low Rayleigh number solutions can be found when $F = O(G) \gg O(1)$. The transformations

$$F = \frac{f}{R_\theta^{1/(1+\alpha)}} \quad \text{and} \quad G = \frac{g}{R_\theta}, \tag{18}$$

can be used in (10), (11) and (13) to show that

$$\frac{dg}{d\eta} = \frac{d}{d\eta}\left[\frac{\cos(\theta_e\eta)}{1+\alpha} f^{1+\alpha}\right] + \frac{\alpha g}{f}\frac{df}{d\eta}, \tag{19}$$

$$\frac{d^2f}{d\eta^2} + \frac{\theta_e^2}{(1+\alpha)^2} f = -\frac{fg}{1+\alpha}, \tag{20}$$

$$f(\eta = 1) = R_\theta^{1/(1+\alpha)}, \quad \frac{df}{d\eta}(\eta = 0) = 0, \qquad R_\theta M = \int_0^1 g\, d\eta. \tag{21a,b,c}$$

Second branch solutions, obtained by quasi-linearization techniques from the lowest-order approximation to (19)–(21), show large thermal effects caused by a special velocity distribution near the origin. Very hot fluid is brought upward in the central portion, while cooler fluid moves downward near the wall. The net mass flux is fixed. A comparison of the two solution branches for $R_\theta \to 0$ is shown in Fig. 2 for $\alpha = 0$, $M = 1$, and $\theta_e = 10°$. Once R_θ is chosen, second branch solutions in terms of F and G can be calculated from (18). It will be convenient to denote the moderate temperature solutions as slug flow type, and those with large temperature variations as jet flow type solutions. The existence of two solutions of (10)–(13) when $R \ll 1$ implies that non-uniqueness may prevail for more general values of R.

High Rayleigh number solutions $(R \to \infty)$ for a slender wedge can be obtained for the limit $R_\theta = O(1)$, $\theta_e \to 0$ when $F = O(G) = O(1)$.

For $\alpha = 0$, the lowest-order terms of (10), (11) and (13) are

$$\frac{dG}{d\eta} = \frac{dF}{d\eta}, \tag{22}$$

$$\frac{d^2F}{d\eta^2} + R_\theta FG = 0, \tag{23}$$

$$F(\eta) = 1) = 1, \quad \frac{dF}{d\eta}(\eta = 0) = 0, \qquad M = \int_0^1 G\, d\eta. \tag{24a,b,c}$$

A first integral of equations (22) and (23) can be written as,

$$\frac{dF}{d\eta} = \pm\sqrt{\tfrac{2}{3}R_\theta}\,[(e_1 - F)(e_2 - F)(e_3 - F)]^{1/2}, \tag{25}$$

where,

$$e_1 + e_2 + e_3 = -A, \text{ a constant}, \tag{26}$$

$$e_1e_2 + e_2e_3 + e_3e_1 = 0. \tag{27}$$

The solution to equation (25) will depend upon whether the roots e_1, e_2 and e_3 are real or complex.

The integration of (25) is obtained in terms of an elliptic function [18] for the real roots e_i. A numerical attempt was made to obtain solutions F and G satisfying boundary conditions (24), for $R = 10$, 20 and 30 with $\theta_e = 10°$ and $M = 1$. No

solution was found which satisfies (24). It appears that solutions to the system (22)–(24) do not exist for real values of e_i. However, a compelling proof, beyond an extensive computer search, is not obvious.

The integration of (25) for complex roots gives

$$F = e_1 - H\frac{1-cn\left[\left(\frac{2R_\theta H}{3}\right)^{1/2}\eta, m\right]}{1+cn\left[\left(\frac{2R_\theta H}{3}\right)^{1/2}\eta, m\right]}, \tag{28}$$

where

$$G = F + \frac{2A}{3}, \tag{29}$$

$$e_1 > 0, \quad e_{2/3} = a \pm ib, \tag{30}$$

$$H^2 = e_1^2 - 2ae_1 + a^2 + b^2, \tag{31}$$

$$m = \frac{H + e_1 - a}{2H}, \tag{32}$$

and cn denotes a standard elliptic function [18].

One may combine (24), (26), (27), (30)–(32) to show that

$$\frac{H^2}{3(M+C)} - H\frac{1-cn\left[\left(\frac{2R_\theta H}{3}\right)^{1/2}, m\right]}{1+cn\left[\left(\frac{2R_\theta H}{3}\right)^{1/2}, m\right]} = 1, \tag{33}$$

$$C = \frac{H}{u}\left[-2E(u) + sn(u)\,dc(u) + u\right], \tag{34}$$

$$u = \left(\frac{R_\theta H}{6}\right)^{1/2}, \tag{35}$$

$$m = \frac{1}{2H}\left[H + \frac{H^2}{4(M+C)} + \frac{3}{4}(M+C)\right], \tag{36}$$

where dc and sn are standard elliptic functions [18].

Equations (33)–(36) are solved for a given R_θ and M. Once H and m are known, equations (28) and (29) are solved for different values η, where

$$e_1 = \frac{H^2}{3(M+C)}, \tag{37}$$

$$\frac{2A}{3} = M - e_1 + C. \tag{38}$$

Here again it is found that the solution to the system (33)–(36) is not unique for a given set of parameters. The two types of solution are shown in Figs. 3 and 4.

The existence of easily-obtained solutions for complex values of e_i lends credence to the belief that solutions do not exist for real e_i.

For wedges of finite included angle, large Rayleigh number solutions ($R \to \infty$) can be obtained for the limit $R_\theta \to \infty$, θ_e fixed. It can be noted that the highest derivative in F is lost in the energy equation (11) for this limit, giving rise to the isothermal slug flow at the cold environmental temperature in the central core region of the wedge. This implies that

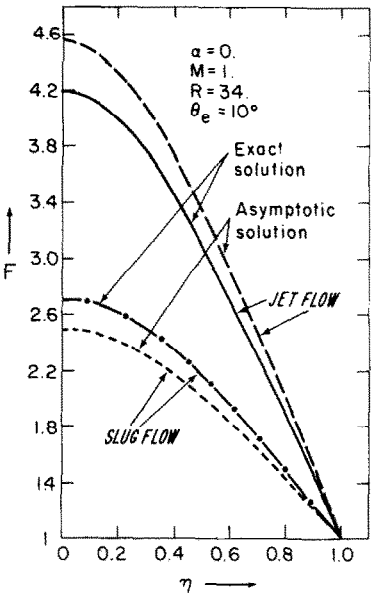

FIG. 3. Asymptotic and numerical temperature (F) solutions for slug and jet type flow: $\alpha = 0$, $M = 1$, $\theta_e = 10°$, $R = 34$.

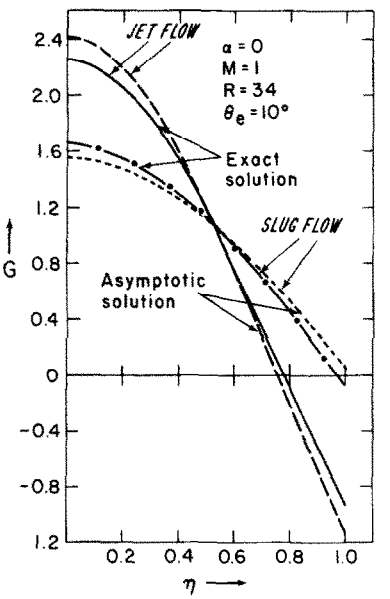

FIG. 4. Asymptotic and numerical velocity (G) solutions for slug and jet type flow: $\alpha = 0$, $M = 1$, $\theta_e = 10°$, $R = 34$.

core flow would be downward from above, or that $M < 0$. This suggests that the solution for $M > 0$ does not exist. This point can also be proved mathematically by using an inner variable to keep the highest derivative in the energy equation (11). It can be seen that the solution to the resulting boundary layer equations does not satisfy the required boundary conditions and hence the diverging flow can not exist for this limit of $R_\theta \to \infty$.

4. NUMERICAL SOLUTIONS

Numerical solutions are the exact solutions obtained by integrating the coupled nonlinear differential equations (10)–(11). The equations were first quasilinearized (Kalaba [8]) and then trial functions for F and G, obtained from the two classes of solutions generated in the asymptotic analysis of complex roots, are used to generate the two distinct numerical solutions. In Figs. 3 and 4, a comparison is made between the lowest-order asymptotic results and the numerical solutions for the parameters shown. It can be seen that the maximum difference in F is about 7.5% for the lower solution, and 9.5% for the upper. It can be noted that both numerical solutions show the existence of the reverse flow regions.

5. RESULTS AND DISCUSSION

Both numerical solutions to (10), (11) and (13) are plotted in Figs. 5 and 6 for several values of R. It is observed that these solutions approach each other as R increases to a limiting value.

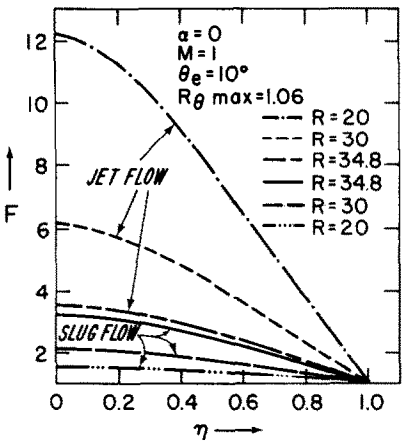

FIG. 5. Effect of Rayleigh number (R) on the temperature (F) for slug and jet type flow: $\alpha = 0$, $M = 1$, $\theta_e = 10°$.

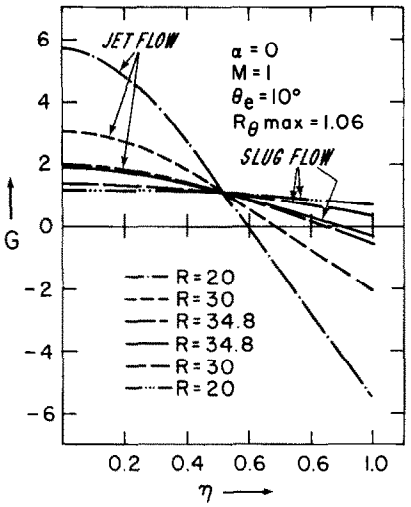

FIG. 6. Effect of Rayleigh number (R) on the velocity (G) for slug and jet type flow: $\alpha = 0$, $M = 1$, $\theta_e = 10°$.

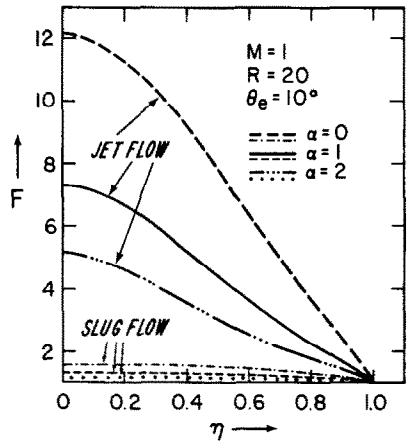

FIG. 7. Effect of the viscosity exponent (α) on the temperature (F) for slug and jet type flow: $M = 1$, $\theta_e = 10°$, $R = 20$.

As the viscosity–temperature relation in equation (5) is changed by varying α, the temperature boundary condition on the wall, defined by equations (8) and (13a), is altered. It follows that a comparison of solutions at different α-values, with all other parameters equal, must be treated with care, because the basic boundary value problems are altered. In Figs. 7 and 8, the effect of α (kinematic viscosity exponent) on the temperatures and velocity profiles is shown. Both solutions show a decrease in temperature with increasing α (decreasing ν). It is clear from (8) and (13a) that an increase in α increases the wall temperatures along the length of the wedge and decreases the temperature gradients there. For a given specified characteristic temperature difference across the wedge, an increase in α would require a corresponding decrease in the heat transfer through the sides of the wedge. Also, the increase in α reduces the local convection effects because the wall temperatures along the wedge tend to be constant. Both of these effects give rise to lower values of F as seen in Fig. 7. Solutions of the jet type flow are more sensitive to α-variations because of the generally larger temperature variations compared to the slug type flow. Velocities are expected to be higher in jet type flow, because of appreciable reduction in the kinetic viscosity. This is unlike the slug type flow with moderate temperatures, in which velocities are not affected appreciably with changing α (Fig. 8).

Figure 9 shows a plot of θ_e vs R_{max} for different values of M and α. Divergent flow, symmetric solutions exist in the regions below the curve in question, but do not exist in the regions above the curve. It can also be seen that R_{max} increases with the decrease in M and θ_e, and with increase in α.

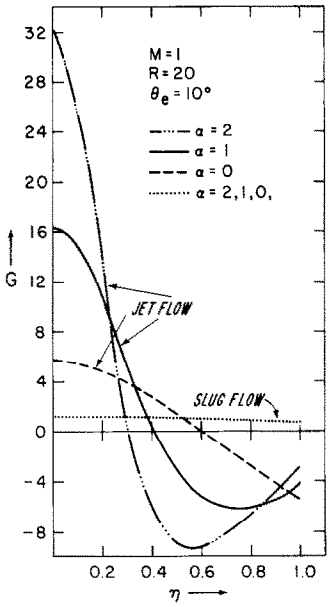

FIG. 8. Effect of the viscosity exponent (α) on the velocity (G) for slug and jet type flow: $M = 1$, $\theta_e = 10°$, $R = 20$.

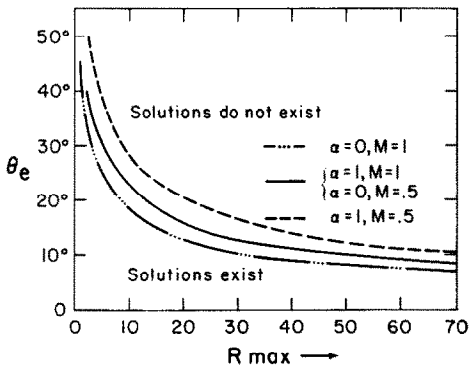

FIG. 9. Effect of viscosity exponent (α) and mass flow rate (M) on the maximum Rayleigh number (R_{max}) for which divergent solutions exist.

In Fig. 10, the similarity wedge centerline velocity $G(0)$ found from numerical computation is plotted as a function of R for $\alpha = 0,2$. Both solution branches are shown. For a given value of R, we note that the slug flow solution shows a decrease in $G(0)$ when α increases. The jet flow solutions display an increase in $G(0)$. It may be observed again that solutions do not exist beyond a certain maximum value of R when other parameters are held constant. The value of maximum R increases with increasing α. The centerline velocity for a jet flow solution is higher for $\alpha = 2$ because of reduced kinematic viscosity. Asymptotic solutions obtained for $R_\theta \to 0$, $F = O(G) \gg 1$, are also plotted for $\alpha = 0$. It may be observed that the two solutions are very close when $R_\theta \to 0$.

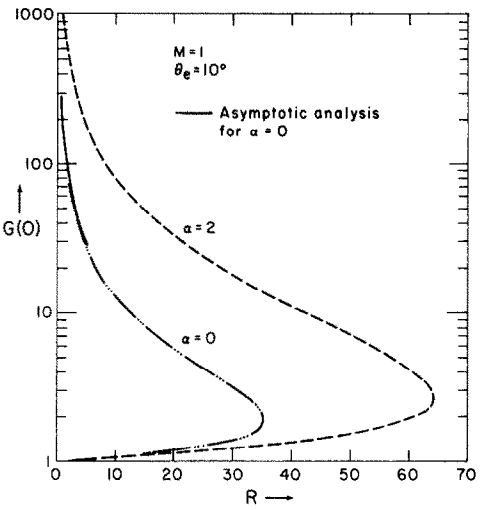

FIG. 10. The wedge centerline velocity $G(0)$ vs Rayleigh number (R) for $\alpha = 0,2$: $M = 1$, $\theta_e = 10°$.

6. APPLICATION TO A HYPOTHETICAL GEOPHYSICAL PROBLEM

Kassoy and Zebib [10] have considered the cooling of a rising column of heated water within a porous medium confined by parallel impermeable boundaries. An application to the heat and mass transfer within a fault zone located in a geothermally active section of the earth's crust was presented. Here, we consider a related application to a slender wedge-shaped fault embedded in the crust of the earth. The theoretical results are applied to the section of the wedge between $r' = L'$ and the radial location at which the wedge intersects the earth's surface in order to avoid the singularity at $r' = 0$.

The following data are assumed:

depth of the fault; $D' = 2\,\text{km}$,
included angle of the wedge; $2\theta_e = 20°$,
temperature at the earth's surface; $T_t' = 25°\text{C}$,
temperature at $r' = L'$; $T_B' = 225°\text{C}$.

Then it follows that the radial distance from the apex to the surface is given by $r_D' = D'/\cos\theta_e = 2.03\,\text{km}$. For the constant viscosity case ($\alpha = 0$), it can be seen from (4c), (8) and (13a) that

$$\Delta T' = (T_B' - T_t')\frac{r_D}{r_D - 1}, \tag{39}$$

where

$$r_D = \frac{r_D'}{L'}. \tag{40}$$

It follows that a relation for L' can be obtained in terms of known quantities from (4f) and (39),

$$L' = \frac{Rr_D'}{R + \dfrac{r_D'}{\gamma}(T_B' - T_t')}, \tag{41}$$

where

$$\frac{1}{\gamma} = \frac{g'\alpha_{e0}'k_0'c_{p0}'\mu_0'}{\nu_0'^2\lambda_{m0}'}. \tag{42}$$

The material properties of liquid water appearing in (42) can be evaluated at the upper boundary of the crust ($T' = 25°C$ and $p' = 1$ atm), in order to find γ. The appropriate values are

$$\begin{aligned} \alpha'_{e0} &= 2.6 \times 10^{-4}/\text{K}, \\ k'_0 &= 10^{-9}\,\text{cm}^2, \\ c'_{p0} &= 4.179 \times 10^7\,\text{cm}^2/\text{s}^2 \cdot \text{K}, \\ \mu'_0 &= 0.891 \times 10^{-2}\,\text{g/cm} \cdot \text{s}, \\ \nu'_0 &= 0.894 \times 10^{-2}\,\text{cm}^2/\text{s}, \\ \lambda'_{m0} &= 20.55 \times 10^4\,\text{g} \cdot \text{cm/s}^3 \cdot \text{K}, \\ \rho'_0 &= 0.9971\,\text{g/cm}^3. \end{aligned} \tag{43}$$

If $R = 20$, then one obtains

$$L' \simeq 0.1594\,\text{km}, \quad \Delta T' \simeq 217\,\text{K}, \tag{44a,b}$$

characteristic convection velocity

$$\frac{\alpha'_{e0}\Delta T' g' k'_0}{\nu'_0} \simeq 0.535\,\text{cm/day}, \tag{45}$$

characteristic mass flow rate

$$M' = 2.97 \times 10^5\,\text{kg/day} \cdot \text{km}. \tag{46}$$

The Rayleigh number, based on D' rather than L', is 251.

The centerline temperature and that at the boundary of the wedge is shown in Fig. 11 as a function of the radial distance from the apex. For a slug type flow, the former is a factor of 1.2 larger than the latter. In contrast, the factor is 5.9 for jet flow. The temperatures, for a variable viscosity ($\alpha \neq 0$) case, will be different quantitatively, but qualitatively similar to those presented in Fig. 11. It is apparent from the graph that the temperatures predicted for a jet flow are unrealistically large for geothermal applications involving the convection of liquid water in rock systems.

A calculation of local pressures at different points along the wedge centerline was made for the comparison with the boiling point curve. As an example the wedge centerline pressures at $r' = 0.3$ km are found to be 165 and 154 atm for the slug and jet type flows respectively. Upon comparing with the boiling point curve, it can be concluded that the boiling does not occur for slug type flows but it does occur for jet flows. This again strengthens our belief that jet type flows will not be observed in the physical situation.

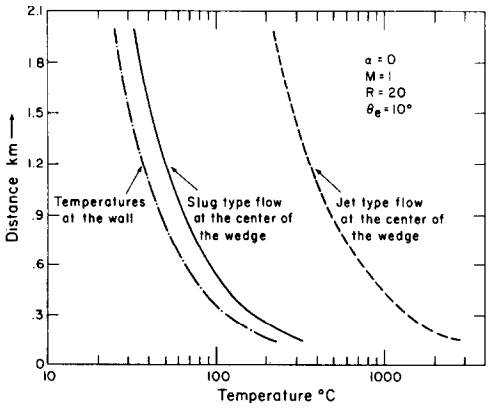

FIG. 11. The dimensional temperature variation with depth in a model fault zone: $\alpha = 0$, $M = 1$, $\theta_e = 10°$, $R = 20$.

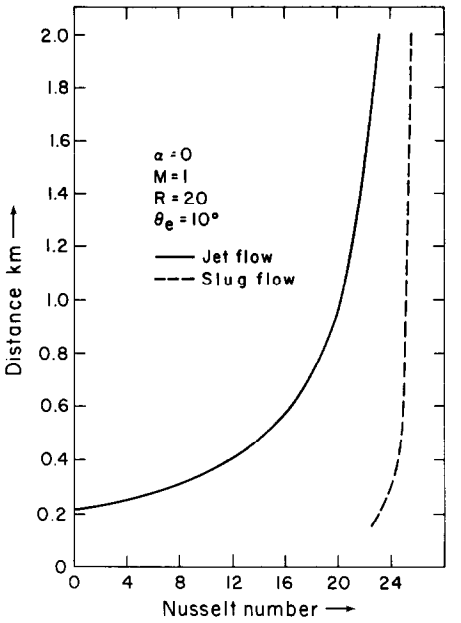

FIG. 12. The Nusselt number (Nu) variation with depth in a model fault zone: $\alpha = 0$, $M = 1$, $\theta_e = 10°$, $R = 20$.

In Fig. 12, the radial Nusselt number, defined as the ratio of the total heat flux across a sector at a given radial distance to the reference heat conduction $2\theta_e b' \lambda'_{m0} \Delta T'$, is plotted as a function of radial distance. The variation for jet type flow is observed to be much larger than the slug flow result. It is noted that the convection process enhances the heat transfer process by a factor of about 25 for the more realistic latter flow.

7. CONCLUSIONS

We have developed exact solutions for the equations which describe diverging radial flow convection of a variable viscosity liquid in a wedge-shaped region of saturated porous medium confined by impermeable walls. It has been shown that the properties of the solutions depend upon the wedge half-angle θ_e, the mass flow rate M, the Rayleigh number R, and the viscosity exponent α. For a given set of parameter values θ_e, M and α, it has been found that two distinct solutions exist below a specific Rayleigh number. Slug flow type solutions exhibit relatively small variations in velocity and temperature across the wedge at any radial location. In most cases, the flow direction is purely unidirectional. Large gradients in velocity and temperature and the presence of reverse flow regions characterize the jet flow type solutions. The latter property implies that a very special velocity distribution is required at the apex of the wedge. In this sense, it would be difficult to observe such a flow in

the laboratory, to say nothing of the geophysical environment. Further consideration of the physical significance of the jet flow would require a spatial stability analysis, such as that described in [10], in order to determine whether such a flow is a stable asymptotic solution to a well-developed parabolic differential equation. On the basis of the presence of extensive reverse flow regions, one may conjecture that instability will be found.

The nonexistence of two-dimensional symmetric radial flow solutions above a specific critical Rayleigh number suggests that: (a) asymmetric solutions, like those considered in [2, 3] should be sought and (b) non-planar flow associated with the influence of natural convection, like that studied in [10], should be considered.

Acknowledgement—This work was supported in part by grant NSF(RANN)AER 74-03429-A03, and by a Department of Energy contract administered by Lawrence Berkeley Laboratory.

REFERENCES

1. W. R. Dean, Note on the divergent flow of fluids, *Phil. Mag. Ser. 7* **18**, 759 (1934).
2. L. E. Fraenkel, Laminar flow in symmetrical channels with slightly curved walls—I. On the Jeffery–Hamel solutions for flow between plane walls, *Proc. R. Soc.* **A267**, 119–138 (1962).
3. L. E. Fraenkel, Laminar flow in symmetrical channels with slightly curved walls—II. An asymptotic series for the stream function, *Proc. R. Soc.* **A272**, 406–428 (1963).
4. K. P. Goyal, Heat and mass transfer in a saturated porous medium with application to geothermal reservoirs, Ph.D. Thesis, University of Colorado, Boulder (1978).
5. G. Hamel, Spiral förmige bewegungen zäher flossigükiten, *Jb. Dt. Math. Ver.* **25**, 34 (1916).
6. W. J. Harrison, The pressure in a viscous liquid moving through a channel with diverging boundaries, *Proc. Camb. Phil. Soc.* **19**, 307 (1919).
7. G. B. Jeffery, Steady motion of a viscous fluid, *Phil. Mag. Ser. 6*, **29**, 455 (1915).
8. R. Kalaba, *Nonlinear Differential Equations and Nonlinear Mechanics*, edited by J. P. Lasalle and S. Lipschitz, p. 97. Academic Press, New York (1963).
9. T. Kármán, *Vorträge aus dem Gebiete der Hydro- und Aero-Dynamik*, p. 150. Innsbruck (1922).
10. D. R. Kassoy and A. Zebib, Convection fluid dynamics in a model of a fault zone in the earth's crust, *J. Fluid Mech.* **88**, 769–802 (1978).
11. V. L. Katkov, *Exact solutions of certain convection problems, PMM* (English version), **32**(3), 489 (1968).
12. P. C. Lu and T. H. Chen, Jeffery–Hamel flows with free convection, in *Proceedings of the Fifth International Heat Transfer Conference, Tokyo, Natural Convection* 5–3, Vol. **III**, pp. 183–187 (2–7 September 1974).
13. K. Millsaps and K. Pohlhausen, Thermal distributions in Jeffery–Hamel flows between nonparallel plane walls, *J. Aeronaut. Sc.* **20**, 187–196 (1953).
14. B. Noble, *Numerical Methods*. Oliver and Boyd, Edinburgh (1963).
15. F. Noether, *Handbuch der Physikalischen und Technischen Mechanik*, Vol. 5, pp. 733–736. Springer, Berlin (1931).
16. L. Rosenhead, The steady two dimensional radial flows of viscous fluid between two inclined walls, *Proc. R. Soc.* **175**, 436 (1940).
17. W. Tollmien, *Grenzschichttheorie Handbuch der Experimental-Physik*, Vol. 4 (Part 1), pp. 241–287. Springer, Berlin (1931).
18. L. M. Milne-Thomson, Jacobian elliptic functions and theta functions, *Handbook of Mathematical Functions*, edited by M. Abramowitz and I. A. Stegun, pp. 569–570. National Bureau of Standards, Washington, D.C. (1965).

TRANSFERT DE CHALEUR ET DE MASSE DANS UN DIEDRE POREUX SATURE AVEC DES FRONTIERES IMPERMEABLES

Résumé—On étudie le transfert de chaleur et de masse dans un écoulement bidimensionnel radial de fluide visqueux à l'intérieur d'un milieu poreux saturé en forme de dièdre.

On utilise des transformations de similitude pour la température, la vitesse et la pression, de façon à réduire les systèmes descriptifs à des équations différentielles ordinaires avec des conditions aux limites en deux points. On obtient des solutions exactes et asymptotiques pour la vitesse et la température. Deux solutions distinctes (écoulement de type jet et écoulement piston) existent pour un système donné de paramètres. Des résultats spécifiques sont présentés pour des petits angles de dièdre. On montre que les solutions symétriques divergentes n'existent pas au dessus d'un nombre de Rayleigh critique. Une application de la théorie à la convection d'eau liquide est présentée pour une aire géothermiquement active.

WÄRME- UND STOFFTRANSPORT IN EINEM GESÄTTIGTEN, PORÖSEN KEIL MIT UNDURCHLÄSSIGEN RÄNDERN

Zusammenfassung—Es wird der Wärme- und Stofftransport bei zweidimensionaler radialer Strömung einer zähen Flüssigkeit durch ein gesättigtes, poröses, keil förmiges Gebiet mit undurchlässigen Wänden untersucht. Ähnlichkeitstransformationen werden für Temperatur, Geschwindigkeit und Druck benutzt, um die beschreibenden Systeme auf gewöhnliche Differentialgleichungen mit Zwei-Punkt-Randbedingungen zu reduzieren. Sowohl exakte als auch asymptotische Lösungen werden für die Geschwindigkeit und die Temperatur erhalten. Es wurde gefunden, daß für einen gegebenen Satz von Strömungsparametern zwei unterschiedliche Lösungen (Strahlströmung und verzögerte Strömung) existieren. Typische Ergebnisse für kleine Keilwinkel werden angegeben. Es wird gezeigt, daß oberhalb einer kritischen Rayleigh-Zahl keine symmetrisch divergierenden Lösungen existieren. Die Anwendung der Theorie auf die Konvektion von flüssigem Wasser im stark vereinfachten Modell einer Verwerfungszone in einem geothermisch aktiven Gebiet wird gezeigt.

ТЕПЛО- И МАССОПЕРЕНОС В НАСЫЩЕННОМ ПОРИСТОМ КЛИНЕ С НЕПРОНИЦАЕМЫМИ ГРАНИЦАМИ

Аннотация — Исследуется тепло- и массоперенос при двумерном радиальном течении вязкой жидкости через насыщенную пористую ограниченную стенками клиновидную область. Для температуры, скорости и давления используются автомодельные преобразования, сводящие систему основных уравнений к обыкновенным дифференциальным уравнениям с двухточечными граничными условиями. Получены как точные, так и асимптотические решения для скорости и температуры. Найдено, что при заданных параметрах имеют место два резко выраженных вида решений (течения типа струйных и ползущих). Представлены результаты для небольших углов раствора клина. Показано отсутствие расходящихся решений при числах Релея выше критического. Для грубой модели аварийной зоны в геотермально активной области приведен пример приложения теории к задаче о конвекции воды.